

Dalton Transactions

Accepted Manuscript



This article can be cited before page numbers have been issued, to do this please use: E. Gabano, M. Ravera, F. Trivero, S. Tinello, A. Gallina, I. Zanellato, M. Gariboldi, E. MONTI and D. Osella, *Dalton Trans.*, 2018, DOI: 10.1039/C7DT04614F.



This is an Accepted Manuscript, which has been through the Royal Society of Chemistry peer review process and has been accepted for publication.

Accepted Manuscripts are published online shortly after acceptance, before technical editing, formatting and proof reading. Using this free service, authors can make their results available to the community, in citable form, before we publish the edited article. We will replace this Accepted Manuscript with the edited and formatted Advance Article as soon as it is available.

You can find more information about Accepted Manuscripts in the [author guidelines](#).

Please note that technical editing may introduce minor changes to the text and/or graphics, which may alter content. The journal's standard [Terms & Conditions](#) and the ethical guidelines, outlined in our [author and reviewer resource centre](#), still apply. In no event shall the Royal Society of Chemistry be held responsible for any errors or omissions in this Accepted Manuscript or any consequences arising from the use of any information it contains.



ARTICLE

The cisplatin-based Pt(IV)-diclorofibrato multi-action anticancer prodrug exhibits excellent performances also in hypoxic conditions.[§]

Received 00th January 20xx,
Accepted 00th January 20xx

DOI: 10.1039/x0xx00000x

www.rsc.org/

Elisabetta Gabano,^{a,*} Mauro Ravera,^a Francesca Trivero,^a Stefano Tinello,^a Andrea Gallina,^a Ilaria Zanellato,^a Marzia B. Gariboldi,^b Elena Monti,^b and Domenico Osella^a

Multi-action cisplatin-based mono- (1) and di-clofibrato (2) Pt(IV) “combo” derivatives were synthesized *via* both traditional and microwave assisted procedures. The two complexes offered very good performances (IC₅₀ values in nanomolar range) on a panel of human tumor cell lines, including the highly chemoresistant malignant pleural mesothelioma ones. Moreover, both 1 and 2 bypass the cisplatin resistance. Indeed, cisplatin and clofibrato, the metabolites of the Pt(IV)→Pt(II) intracellular reduction, proved to act synergistically. The adjuvant action of clofibrato relies on the activation of peroxisome proliferator-activated receptor α (PPARα) that, in turn, decreases the level of Hypoxia-Inducible Factor-1α. Both compounds induced extensive apoptosis in tumor cells, also via oxidative stress. Finally, 2 exhibited excellent performances also under the hypoxic conditions typical of solid tumors, where cisplatin is less effective.

Introduction

Although targeted- and immuno- therapies are nowadays considered among the most promising developments in fighting cancer, conventional cytotoxic chemotherapy, in particular the Pt-based one, still represents the first-line armory against very aggressive cancers.

In principle, there are many opportunities to target and kill cancer cells, because they use multiple and redundant pathways to survive. The simplest approach to a simultaneous attack on different molecular targets/mechanisms is the combination chemotherapy, where two or more drugs act in additive or (better) synergistic way. To improve patient compliance, different drugs are incorporated into the same formulation; however, combining multiple medicaments in a single preparation can be challenging, because of pharmacokinetic differences between the individual components. Alternatively, a single chemical entity, containing highly integrated different pharmacophores, can be designed.¹

In this context, the well-established Pt(IV) chemistry permits to design dual- or even multi-functional drug candidates that act as combination-therapy single-molecule, called “combo”.²⁻⁶ One or two adjuvant/synergistic agents (generally containing carboxylic functions) can be conjugated to the octahedral Pt(IV) assembly (generally based on the cisplatin square-plane scaffold) in axial positions. These Pt(IV) derivatives are considered *prodrugs*, because they can reach tumor cells in their intact form and then can be reduced in the hypoxic (reducing) intracellular *milieu* to cytotoxic cisplatin, with the simultaneous loss of the two axial ligands (*activation by reduction*).⁶⁻⁹ Importantly, Pt(IV) complexes are generally much more lipophilic than their progenitors, *i.e.* hydrophilic cisplatin and amphiphilic carboxylate anions (at physiological pH). This means that their assembly permits a more efficient cellular uptake (*via* passive diffusion) than that of the separate components (*synergistic cellular accumulation*).¹⁰

The auxiliary drug selected for the present work is (2-(*p*-chlorophenoxy)-2-methylpropionic acid (clofibrato, CA). Fibrates are widely used in the treatment of dyslipidemia. The CA mechanism of action relies on activation of peroxisome proliferator-activated receptor α (PPARα), a member of the PPAR nuclear receptor superfamily. PPARα controls the fatty acid metabolism. Interestingly, PPARα agonists have been reported to activate apoptotic cell death in different cancer cell lines through different and sometimes contrasting biochemical mechanisms.¹¹ In particular, a brief report claimed (*data not shown in such a paper*) that combination treatment

^a Dipartimento di Scienze e Innovazione Tecnologica, Università del Piemonte Orientale, Viale Michel 11, 15121 Alessandria, Italy. E-mail: elisabetta.gabano@uniupo.it

^b Dipartimento di Biotecnologie e Scienze della Vita, Università dell'Insubria, Via Manara 7, 21052 Busto Arsizio (VA).

[§] presented at XVII Workshop on Pharmacobiometallics, Naples (Italy), on 17 February 2018.

Electronic Supplementary Information (ESI) available: details of the chemical and biological characterization of the compounds under investigation. See DOI: 10.1039/x0xx00000x

in vivo with CA and cisplatin produces efficient antitumor effects on ovarian cancer cells.¹²

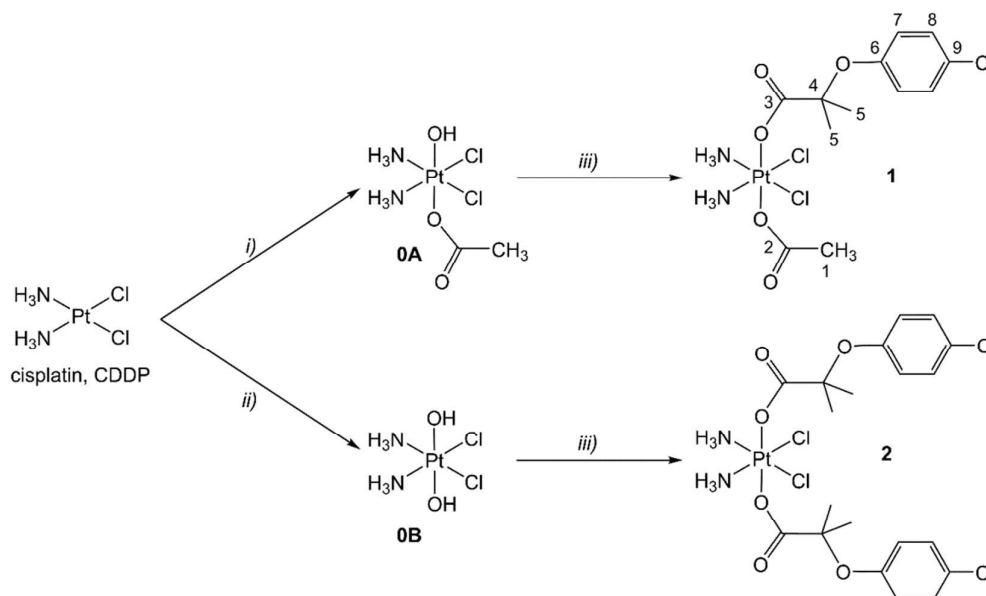
Furthermore, the activation of PPAR α by CA is able to promote the degradation of Hypoxia-Inducible Factor-1 α (HIF-1 α),¹³ the oxygen-dependent subunit of the transcription factor HIF-1, that acts as the master regulator of cellular adaptation to hypoxia.¹⁴ HIF-1 activation has been implicated in solid tumor progression,¹⁵ as well as in poor response to several chemotherapeutic protocols, including those employing cisplatin.¹⁶ Very recently, some Pt(IV) complexes with indazole-based axial ligands, specifically targeting HIF-1 α , exhibited moderately improved anticancer activity in hypoxic with respect to normoxic conditions.¹⁷ The finding that clofibrates induce PPAR α activation and thus promote HIF-1 α degradation suggests that combo Pt(IV)-CA mono- and di-derivatives could offer interesting performances under hypoxic conditions.

In principle, the activity of all the Pt(IV) complexes should be favored by the hypoxic microenvironment encountered in solid tumors. Indeed, the reduction Pt(IV) \rightarrow Pt(II) should be promoted under hypoxic (reducing) conditions, even if the activity of the generated Pt(II) metabolite will be subsequently hindered in the same milieu.¹² The relationship between hypoxia and cytotoxicity of Pt(IV) prodrugs has not been extensively investigated so far. However, in a seminal paper Hambley *et al.* reported that in monolayer (2D) and tumor

spheroid (3D) cultures obtained from non-small cell lung cancer cells the cytotoxicity of cisplatin-based Pt(IV) complexes was unaffected (but not increased) under hypoxic conditions.¹⁸ More recently, Keppler *et al.* showed that the antiproliferative potency is almost identical in normoxic and hypoxic conditions for most of the Pt(IV) derivatives and in most of the 2D and 3D cell lines investigated.^{19, 20}

Noteworthy, renal dysfunction, that is an important adverse effect of cisplatin, was attenuated by co-treatment with fibrates, albeit in doses much higher than that released from the combo derivatives **1** and **2** (Scheme 1).^{21, 22}

In this context, one clofibrate and one acetate (compound **1**) or two clofibrates (compound **2**) were coordinated as axial ligands in the Pt(IV) octahedral scaffold, completed with two ammonia molecules and two chlorides (cisplatin-based Pt(IV) derivatives) (Scheme 1). These compounds were tested *in vitro* on several human tumor cell lines having different chemosensitivity (ovarian, testis, lung, colon, and breast cancer cells). Additionally, several malignant pleural mesothelioma (MPM) cell lines were also tested. Moreover, the occurrence of synergy between cisplatin and CA was verified *in vitro* by means of the combination index (CI) procedure. Finally, additional experiments were carried out using the most active compound **2** on two selected cell lines (namely A2780 and HCT 116) under normoxic and hypoxic conditions.



Scheme 1. Synthetic pathways for compounds **1** and **2**: *i*) H₂O₂ in CH₃COOH (RT, 3–4 h); *ii*) H₂O₂ in H₂O (microwave heating, 70 °C, 20 min); *iii*) clofibril chloride (in acetone + pyridine, reflux overnight or microwave heating 55 °C, 1 h). The numbering scheme for the identification of the NMR signals is reported.

Results and Discussion

Synthesis and characterization of Pt(IV) complexes

All the complexes under investigation were synthesized starting from (*SP*-4-2)-diamminedichloridoplatinum(II)

(cisplatin or CDDP), prepared according to the Dhara's method.^{23, 24} Cisplatin was oxidized to the mono- and dihydroxido intermediates **OA** and **OB**, using hydrogen peroxide in acetic acid or in water, respectively.^{25, 26}

The following step of the syntheses involves the substitution reaction of the axial hydroxido/s with the carboxylic acid/s. However, to perform the substitution

reaction, a more reactive form of CA is necessary and, therefore, this acid was turned into its corresponding clofibroyl chloride using oxalyl dichloride in the presence of a catalytic amount of dimethylformamide, DMF. The reaction between **OB** and clofibroyl chloride was more complicated than that employing **OA**, being the solubility of final complex and unreacted CA very similar. This problem required slight modification of the usual synthetic procedure (see Experimental section).

Furthermore, in the present work, the microwave heating was applied to the synthesis of **OB**, **1**, and **2** with neat advantage in terms of speed, maintaining or even improving yield and purity of the traditional syntheses (see Experimental section). In the field of Pt compounds, the microwave-assisted heating is rather unexplored. The successful application in this work is in tune with the few literature data reporting that microwaves can speed up and/or make possible reactions that hardly occur when thermally driven.^{23, 27-30}

Complexes **1** and **2** were also obtained starting from ¹⁵NH₃-labeled cisplatin.³¹ These ¹⁵N-containing complexes are extremely useful to follow the reduction reactions of the Pt(IV) prodrugs challenged with cytosolic extract.^{8, 26, 32} According to Gibson *et al.*, this test seems to be more realistic than the common kinetic study with models of bio-reductants such as glutathione or ascorbic acid, since the *in vivo* reduction of Pt(IV) complexes seems to be mainly mediated by cytosolic macromolecules.^{8, 32, 33}

Finally, **1** and **2** were characterized by RP-HPLC-ESI-MS and multinuclear (¹H, ¹³C, ¹⁹⁵Pt and ¹⁵N) NMR spectroscopy using both mono- and bi-dimensional techniques, such as heteronuclear single quantum coherence spectroscopy (HSQC), to assign the whole set of signals (ESI contains the most relevant mono- and bi-dimensional NMR spectra). In general, the ¹H and ¹³C NMR spectra of the Pt complexes show a high-frequency shift of the signals of the atoms nearer to the metal center with respect to the free ligands, pointing out the occurred coordination.

¹⁹⁵Pt and ¹⁵N NMR spectroscopy provides information on the oxidation state of the metal and on the nature of the coordinated ligands.³⁴⁻³⁸ Accordingly, the ¹⁹⁵Pt NMR signals of **1** and **2** exhibit chemical shifts around 1050-1250 ppm well-suited with the presence of two chlorides, two carboxylates and two amines coordinated to Pt(IV) in an octahedral geometry.^{26, 39-41} The ¹⁵N NMR signals of ¹⁵N-labeled complexes **1** and **2** exhibit chemical shifts around -40 ppm compatible with the presence of chlorides *trans* to ¹⁵NH₃ in Pt(IV) complexes.^{38,36}

Solution behavior and reduction

Complexes **1** and **2** proved to be stable towards hydrolysis in HEPES buffer (HEPES = 4-(2-hydroxyethyl)-1-piperazineethanesulfonic acid, pH = 7.5) with methanol as a co-solvent for one week at 37 °C, as verified by means of HPLC-MS (see Experimental for details).

The reduction of ¹⁵N-labeled complexes **1** and **2** was followed by ¹⁵N NMR spectroscopy using cell extracts from A2780 ovarian cancer cells (see ESI, Figures S16-S19). After 30

min of incubation, the [¹H, ¹⁵N] HSQC spectra showed the absence of the original signals of Pt(IV) complex (¹⁵N-**1** δ = -40.3 ppm and ¹H δ = 6.4 ppm; ¹⁵N-**2** δ = -39.8 ppm and ¹H δ = 6.4 ppm) and the presence of that of cisplatin (¹⁵NH₃ δ = -67.0 ppm with satellite peaks at -63.7 ppm and -70.2 ppm, ¹J_{Pt-N} = 330 Hz and ²J_{Pt-H} = 64 Hz; ¹H δ = 4.0 ppm).

Antiproliferative activity and synergism

The half-maximal inhibitory concentrations, IC₅₀, were determined on a panel of human cancer tumor cells. Ovarian A2780, testis NT2/D1, lung A549, colon HCT 116, breast MCF7 cancer cells, together with five malignant pleural mesothelioma cells (BR95, MG06, MSTO-211H, and MM98, the latter both as wild type and cisplatin-resistant subline MM98R) were challenged with **1** and **2**, along with cisplatin and CA for comparison purpose (Table 1).

Table 1. Antiproliferative data (IC₅₀) of cisplatin, CA, and Pt(IV) complexes **1-2** (72 h continuous treatment, CT, normoxic conditions: 21% O₂). The panel of cancer cell lines includes: ovarian carcinoma A2780, testicular cancer metastatic cell tumor NT2/D1, lung carcinoma A549, colorectal cancer HCT 116, breast adenocarcinoma MCF7, and five malignant pleural mesotheliomas (epithelioid phenotypes BR95 and MG06, biphasic MSTO-211H, sarcomatoid MM98, and its cisplatin-resistant subline MM98R). Data are reported as means ± standard deviation of at least three independent replicates.

Cell lines	IC ₅₀ [μM]			
	Cisplatin	CA	1	2
A2780	0.5 ± 0.1	(1.0 ± 0.2) × 10 ³	0.081 ± 0.006	0.028 ± 0.006
NT2/D1	0.11 ± 0.05	(2.8 ± 0.6) × 10 ³	0.031 ± 0.002	0.022 ± 0.008
A549	3.6 ± 0.9	(1.4 ± 0.3) × 10 ³	0.86 ± 0.03	0.12 ± 0.04
HCT 116	2.3 ± 0.3	(1.2 ± 0.2) × 10 ³	0.31 ± 0.08	0.042 ± 0.009
MCF7	6.5 ± 0.9	(1.4 ± 0.2) × 10 ³	1.1 ± 0.1	0.26 ± 0.02
BR95	6.2 ± 0.9	(0.95 ± 0.03) × 10 ³	1.66 ± 0.06	0.44 ± 0.06
MG06	4.1 ± 1.5	(1.6 ± 0.6) × 10 ³	2.6 ± 0.2	0.5 ± 0.1
MSTO-211H	1.4 ± 0.3	(1.0 ± 0.4) × 10 ³	0.4 ± 0.2	0.041 ± 0.007
MM98	3.2 ± 1.0	(4.6 ± 0.9) × 10 ³	1.49 ± 0.09	0.23 ± 0.05
MM98R	19.4 ± 2.8	(3.6 ± 0.3) × 10 ³	1.7 ± 0.5	0.24 ± 0.02
RF ^a	6.1	0.8	1.2	1.0

^a resistance factor RF = IC₅₀(MM98R) / IC₅₀(MM98)

CA showed a modest antiproliferative activity when employed as a single agent, with millimolar IC₅₀ values on all the cell lines tested. On the contrary, cisplatin exhibited IC₅₀ values in the low micromolar range, whereas **1** and **2** were one-two orders of magnitude more active than cisplatin, depending on the chemosensitivity of the cell type. Both **1** and **2** were able to bypass cisplatin resistance with resistance factors (RF = IC₅₀(MM98R) / IC₅₀(MM98) near to 1. While the antiproliferative potency of **1** is similar to that of the mixture of free drugs, the antiproliferative potency of **2** is much higher (Figure 1a), in tune with a higher cellular accumulation (see later).

The evaluation of the pharmacological interaction between the two metabolites produced by reduction into the cells, cisplatin and CA, was performed by using the combination index (CI).^{44, 45} This method evaluates the effect of two (or more) drugs and quantifies synergism or antagonism by determining how the combination effect differs from the

simple additive effect. The *CI* equation, which considers both the potency and the shapes of the dose-effect curves, is used to precisely understand drug combinations: $CI \cong 1$ indicates an additive effect, $CI < 1$ and a $CI > 1$ indicate synergism and antagonism, respectively (see Experimental section).

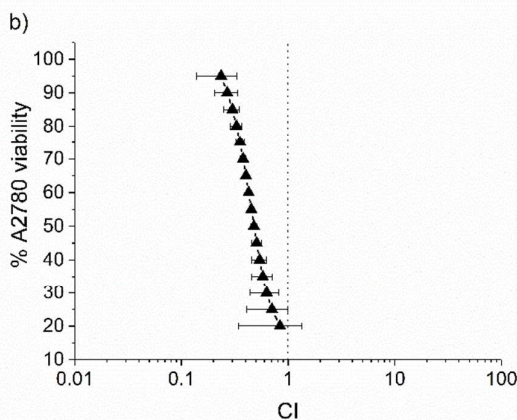
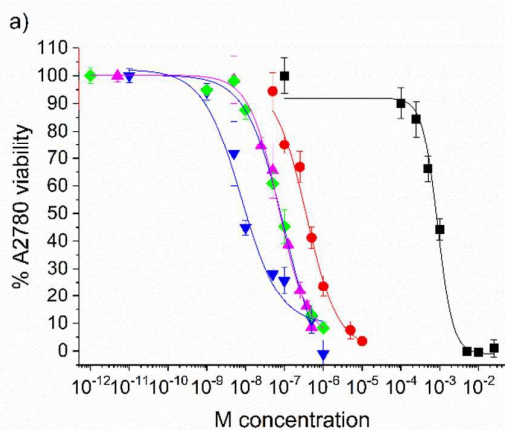
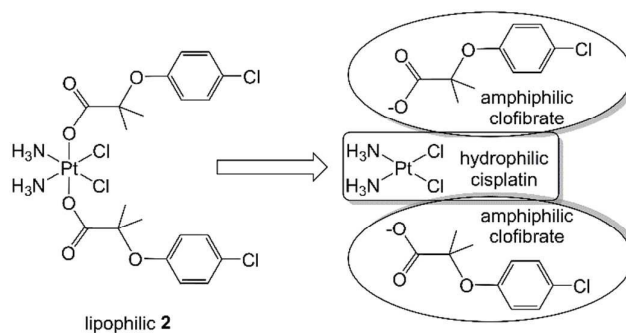


Figure 1. a) Concentration–response curves of A2780 cells challenged for 72 h with CA (black squares), cisplatin (red dots), mixture 1:1000 cisplatin/CA, (magenta upward triangles), **1** (green diamonds), **2** (blue downward triangles). Data are means \pm standard deviation of a representative experiment. Residual viability was assessed by means of the resazurin reduction assay and data were fitted with a four-parameter sigmoidal function (black, red, magenta, green and blue lines, respectively). b) Combination index (CI) plot of the mixture 1:1000 cisplatin/CA. Residual viability data were compared to those obtained for cisplatin and CA to obtain the value. ($CI < 1$: synergism; $CI \cong 1$ additive effect; $CI > 1$ antagonism).

Figure 1b clearly indicates that cisplatin and CA have a synergistic action in the whole range of concentrations employed, so that the two metabolites released within the cells by the Pt(IV) complexes increase each other's effectiveness.

The employed mixture of the free drugs is in 1:1000 cisplatin/CA ratio according to their IC_{50} values (Table 1 and Figure 1). However, it has been previously shown that bioactive carboxylic acids, such as valproic acid (VPA) present as amphiphilic carboxylate at physiological pH, barely enter cells. Indeed the intracellular concentration is about 3 orders of magnitude lower than that originally administered.⁴²

Therefore, the high concentration of such a drug is essential to guarantee its active intracellular level. On the contrary, when the two drugs, *i.e.* hydrophilic cisplatin and amphiphilic clofibrate, are ideally assembled in a lipophilic Pt(IV) scaffold (Scheme 2), synergistic accumulation into the cells can be exploited.^{42, 43} For this reason, complexes **1** and **2** have behaviour similar to or even better than the mixture of free cisplatin and CA (Figure 1a).



Scheme 2. The lipophilic complex **2** may be regarded as the combination of hydrophilic and amphiphilic moieties.

Apoptosis induction

It is well recognized that the failure of many chemotherapeutic treatments arises from the inability to induce apoptosis in cancer cells. The adducts formed by DNA-platination produce the sequential activation of several signal transduction pathways that culminate in apoptotic cell death.^{46, 47} The induction of apoptosis (both *via* intrinsic and extrinsic pathway) is generally associated with the activation of caspases 3 and 7. Therefore, the measurement of their activity is a convenient way to assess whether the cells are undergoing apoptosis concomitant to proliferation arrest. To elucidate if **1** and **2** induced apoptosis in A2780 cells, the caspase 3/7 activity was measured with a DEVD-based fluorogenic assay (DEVD = Asp-Glu-Val-Asp). Figure 2 shows the activity of caspase 3/7 when the A2780 cells are challenged with **1**, **2**, cisplatin, and CA at increasing concentrations. The ability of activation of caspase 3/7 was in the order: **2** > **1** > cisplatin >> CA. Thus, the di-CA complex **2** was able to trigger apoptotic cell death more effectively than the mono-CA complex **1** and cisplatin.

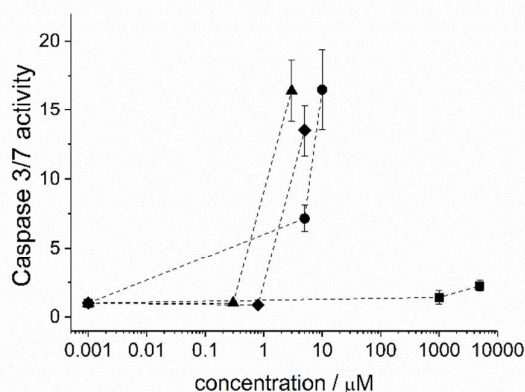


Figure 2. Caspase-3/7 activity (fold increase) of A2780 cells treated with CA (squares), cisplatin (dots), **1** (diamonds), **2** (triangles). Data, normalized to untreated control and residual viability, are means \pm standard deviations of three experiments performed in triplicate.

Apoptosis is characterized by chromatin condensation in early phases and later by nuclear fragmentation.⁴⁸ Accordingly, an increasing number of A2780 nuclei characterized by Hoechst 33342 (a DNA intercalating dye) fluorescence was observed after 24 h in the order **2** > **1** > CA (10 μ M **1** and **2**, and 1 mM CA; Figure 3). In addition, a relevant fraction of nuclear fragmentation (nuclei with the typical punctuate morphology) was observed only as a consequence of treatment with **2**, in tune with caspase activity (Figure 2).

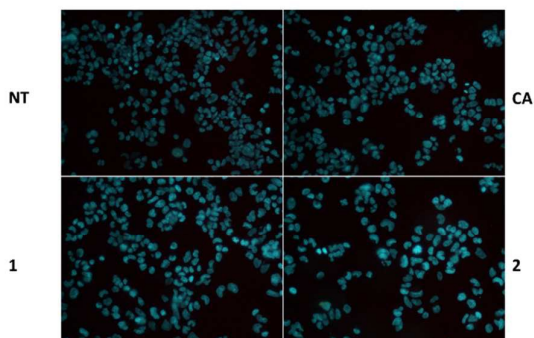


Figure 3. Chromatin condensation and fragmentation of A2780 cell nuclei following 24 h (1 mM CA or **1** or **2**), along with the untreated control (NT). Pictures were taken by a fluorescent microscope (standard DAPI filters, 200X magnification) on living cells immediately after Hoechst 33342 staining.

Lipophilicity, cell uptake and DNA platination

It has been reported that Pt(IV) complexes enter cells mainly (if not exclusively) by passive diffusion.⁴⁹ For this reason, lipophilicity is a key feature for such a process. In a first attempt to determine the lipophilicity of the complexes under study, the traditional octanol-water shake-flask method was employed, but the rather low water solubility of the complexes prevented the achievement of reliable and reproducible data. Therefore, this method was substituted using both a HPLC procedure and *in silico* calculations. RP-HPLC techniques are often used to measure the lipophilicity of a compound, since

the retention is due to partitioning between the C18 chains of the stationary phase (representing the cellular membrane) and the aqueous eluent (representing the water inside and outside cells).^{40, 50} The retention times (t_R) of the complexes were determined on a C18 column by using a 30% aqueous formic acid (15 mM) / 70% MeOH mixture as an eluent and the data were expressed as $\log k'$ ($k' = (t_R - t_0) / t_0$, where t_0 is the column dead-time). Recently, some models for the prediction of the $\log P_{o/w}$ values for both Pt(II) and Pt(IV) complexes have been developed and made publicly available. The final and recommended model (**ASNN5 model, <http://ochem.eu/article/76903>) was here applied to the studied Pt complexes.⁵¹ Finally, the Pt(IV) complexes were tested for their solubility in water. Data are reported in Table 2.

Table 2. Solubility and lipophilicity data.

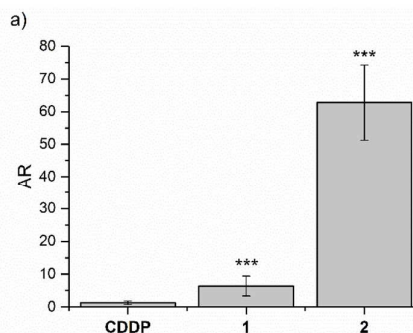
Complex	Solubility [mM]	$\log k'$	Calculated $\log P_{o/w}$
cisplatin	7.7 ^a	-0.50	-2.0 (experimental value -2.13) ^b
1	0.44	0.19	0.49
2	0.01	0.88	1.97

^a apparent water solubility;⁵² ^b mean experimental value of shake-flask literature data.⁵³⁻⁵⁷

As expected, solubility and lipophilicity are inversely correlated and in tune with the chemical structures of the complexes.

The intracellular Pt accumulation of **1** and **2** was measured as a key parameter in understanding the mechanism of action of the complexes. This parameter, that is the final balance between cellular influx and efflux,⁵⁸ is here expressed as accumulation ratio (AR), the ratio between the intracellular Pt concentration and the extracellular (in the culture medium) Pt concentration at a given time.⁵⁹ The AR values were measured on A2780 cells after 4 h of continuous treatment (CT) with 10 μ M concentrations of the Pt compounds (Figure 4). The AR trend is in agreement with the lipophilicity data.

Finally, the platination of genomic DNA, expressed as pg Pt μ g⁻¹ DNA, is reported in Figure 4. By comparing Figure 4a and Figure 4b it is clear that the DNA platination, and hence the antiproliferative potency, is roughly proportional to the cellular accumulation.



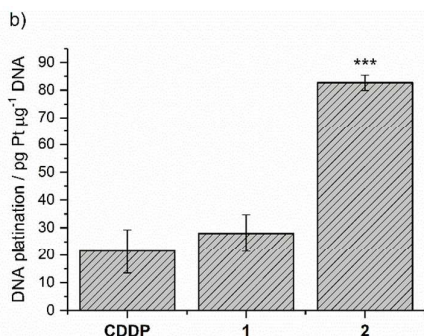


Figure 4. a) Accumulation ratio, AR, and b) DNA platinumation measured on A2780 ovarian cancer cells after treatment with 10 μM concentrations of cisplatin (CDDP) and complexes **1** and **2** for 4 h of continuous treatment. Data are means \pm standard deviations of three experiments performed in triplicate and were compared to cisplatin by means of a two-tailed *t*-test (* $p < 0.05$; ** $p < 0.01$; *** $p < 0.001$).

Gene modulation

In order to shed more light on the biochemical mechanisms operating for **1** and **2**, a quantitative polymerase chain reaction, by reverse transcription quantitative PCR (RT-qPCR) analysis, was carried out. With the aim to perform equitoxic treatments, the IC_{50} values were calculated from the corresponding dose-response curves (24 h CT) of **1**, **2**, along with free CA and cisplatin.

It was shown that CA activates PPAR α in A2780 cells.⁶⁰ This transcription factor upregulates target genes, such as acyl-CoA

oxidase 1 (ACOX1) and carnitine palmitoyltransferase 1A (CPT1A), the key players of fatty acid oxidation.⁶¹ Figure 5 shows that all the Pt complexes induced a striking increase ($p < 0.001$ vs. control) of ACOX1 and CPT1A. For ACOX1, the results seem to indicate the primary role of CA, as far as gene upregulation increases from 12 for cisplatin to about 27 for **1** and **2**. In addition, the modulation of genes ruling the antiproliferative and cytotoxic activity (cyclins (A, E, and D1), p53, and p21) was also investigated. A strong upregulation of cyclins was observed following treatment with cisplatin (Figure 5). This effect was not balanced by the (expected, but limited)⁶² downregulation induced by CA in **1** and **2**. Thus, both Pt(IV) compounds showed a cyclin upregulation similar to that of cisplatin. The strong upregulation of p53 confirms this observation.

On the contrary, p21 was upregulated in the order **2** > **1** > cisplatin > CA, *i.e.* the same trend observed for apoptosis induction. In fact, the expression of p21 increases in response to DNA damage, that induces cell cycle arrest.⁶³

Another gene expected to be upregulated by CA treatment is heme oxygenase (HMOX1), albeit in a PPAR α -independent way.⁶⁰ Figure 5 shows that HMOX1 was strikingly upregulated also by cisplatin, but, to a larger extent, by the combos **1** and **2**. Since this gene is usually increased by oxidative stress, reactive oxygen species (ROS) were evaluated in the same time interval (24 h).

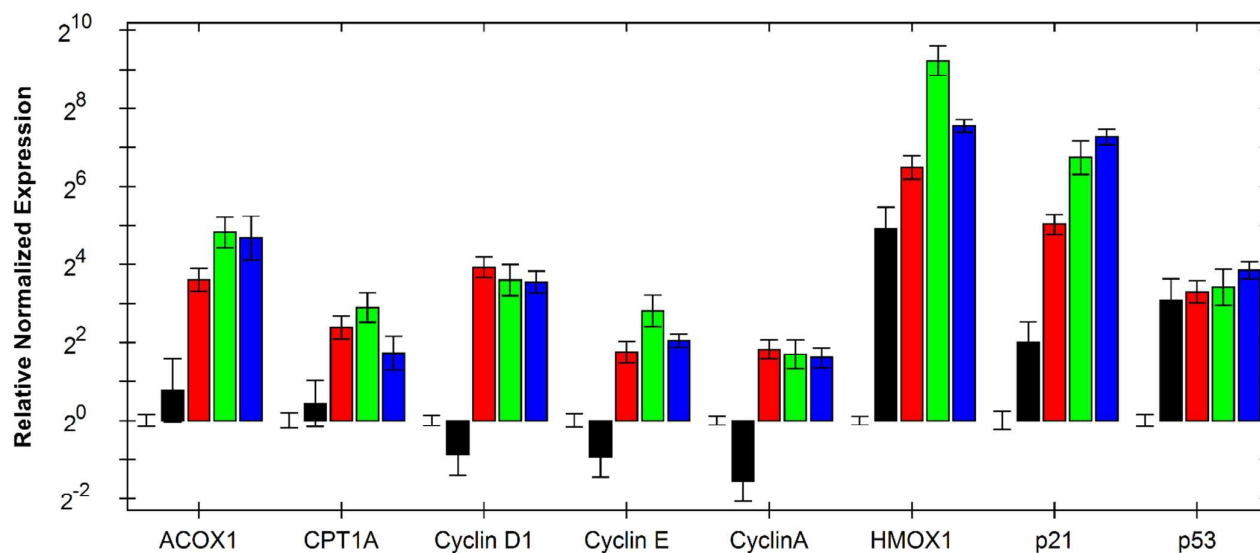


Figure 5. Relative gene expression of ACOX1, CPT1A, Cyclin D1, E, A, p21, p53, HMOX1 in A2780 cells following equitoxic 24 h treatments with CA (5 mM, black bars), cisplatin (30 μM , red bars), **1** (6 μM green bars), **2** (2 μM blue bars). The RT-qPCR experiment was performed in triplicate, and results were normalized to reference genes and untreated control (white bars). All data are means \pm standard deviations and were compared to untreated control by means of a one-way ANOVA test (at least $p < 0.05$, except ACOX1 and CPT1A after CA treatment).

ROS induction

The levels of ROS were measured by means of the dichlorofluorescein diacetate (DCF) assay. Figure 6 shows a

negligible increase of ROS after CA treatment. On the contrary, treatment with Pt complexes increased ROS in the order

1 > **2** \cong cisplatin, ⁶⁴ in tune with the trend of HMOX1 expression.

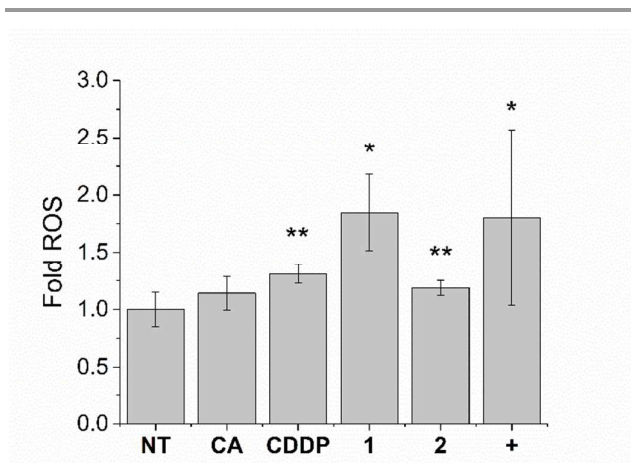


Figure 6. Fold ROS induction compared to untreated control (NT). A2780 cells were treated with 1 mM CA, 1 μ M cisplatin (CDDP), **1**, and **2** for 24 h. H₂O₂ (+) was used as positive control of the DCF assay. Data are means \pm standard deviations (n = 5) and were compared to control by means of a one-way ANOVA test with Dunnett's post test (* p < 0.5; ** p < 0.01; *** p < 0.001).

Hypoxia vs. normoxia

Being **2** the most potent of the two newly synthesized compounds, the following biological tests were limited to it.

Table 3. Antiproliferative effect of CA, cisplatin and **2** on A2780 and HCT 116 cells following 48-h exposure under normoxic or hypoxic conditions. IC₅₀ values are the means \pm standard error mean of 3-5 independent experiments.

Cell lines	IC ₅₀ [μ M], 48 h								
	CA			Cisplatin			2		
	normoxic	hypoxic	ratio	normoxic	hypoxic	ratio	Normoxic	hypoxic	ratio
A2780	(5.3 \pm 0.6) $\times 10^3$	(8.7 \pm 0.2) $\times 10^3$	1.6	1.7 \pm 0.6	5.4 \pm 0.9	3.2	0.05 \pm 0.02	0.03 \pm 0.02	0.6
HCT 116	(6.2 \pm 0.7) $\times 10^3$	(5.1 \pm 0.1) $\times 10^3$	0.8	12 \pm 5	22 \pm 5	1.9	0.4 \pm 0.1	0.3 \pm 0.1	0.7

As mentioned above, tumor hypoxia leads to chemoresistance in many, but not in all tumor cell lines.^{13, 19, 65-73} This can be related to an increased expression and activity of hypoxia-induced HIF-1 α , a well-known regulator of tumor growth, angiogenesis, and metastasis. Treatment with CA and other fibrates is able to diminish HIF-1 α , restoring chemosensitivity.¹³

The influence of hypoxia was evaluated by assessing the viability of A2780 and HCT 116 cells following exposure to the more active compound **2** and to the reference parent compounds cisplatin and CA, under normoxic (21% O₂) or hypoxic (1% O₂) conditions. Preliminary control experiments indicated that the maximum period of hypoxia well tolerated by these cells is 48 h. Accordingly, the IC₅₀ values were calculated from the corresponding dose-response curves (48 h CT) and reported in Table 3. Obviously, compared to the standard treatment time (72 h CT), the potency is lower (higher IC₅₀), as expected for genotoxic drugs that require some population doubling times for working at the best. A 2-3 time increase of IC₅₀ was observed on passing from normoxic to hypoxic conditions for cisplatin. On the contrary, **2** exhibits moderately better performances on both cell lines in hypoxic when compared to normoxic conditions.

Evaluation of the percentage of apoptotic cells was carried out on the same cell lines after 48 h CT with cisplatin and **2** by flow cytometric analysis (Figure 7).

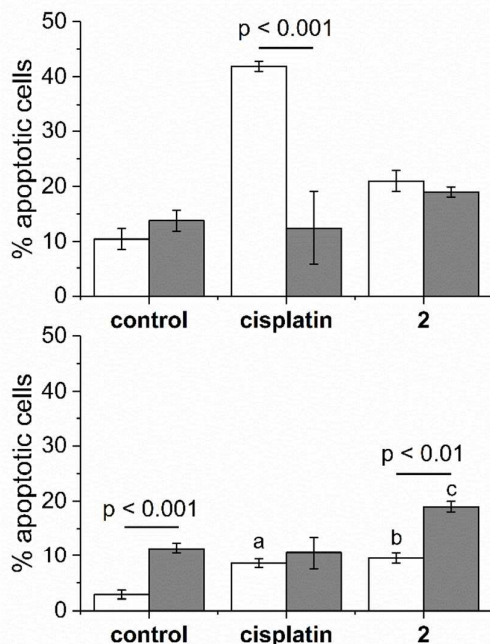


Figure 7. Flow cytometric assessment of the percentage of apoptotic A2780 (top) and HCT 116 (bottom) cells following 48-h CT under normoxic (white bars) and hypoxic (grey bars) conditions with cisplatin and **2** at their respective normoxic IC_{50} values. Values are the means \pm standard error means of 2-4 independent experiments. a: $p < 0.05$ vs. control; b: $p < 0.01$ vs. control; c: $p < 0.01$ vs. control and cisplatin.

In ovarian A2780 cells, cisplatin induced a significant increase of apoptotic cells under normoxic, as compared to hypoxic conditions. On the contrary, no significant differences in apoptosis between normoxic and hypoxic conditions were observed for **2**. The HCT 116 cell line exhibits a different behavior: *i*) a smaller increase in apoptosis cells was observed in response to cisplatin treatment, a well-known phenomenon that can be attributed to a deficit in mismatch repair in this cell line;⁷⁴ *ii*) a significant increase in apoptotic cells was observed when **2** was employed in hypoxic conditions.

Cell cycle analysis (Fig. S20, see ESI) indicates that **2** significantly increased the percentage of cells in G2/M as compared to control and cisplatin, with a corresponding decrease of the G1 sub-population in both A2780 and HCT 116 cells under normoxic conditions. This behavior was maintained in HCT 116 cells following hypoxic incubation. Except for this, cell distribution throughout the different phases was substantially unaffected by oxygen levels.

The ability of the released CA to decrease HIF-1 α level was verified by Western blot analysis after equitoxic treatments of CA, cisplatin and **2** under hypoxia. Figure 8 indicates that **2** induced a more marked degradation of HIF-1 α , with respect to the references, as expected for the synergistic contribution of cisplatin and CA. This effect explains the ability of **2** to work under hypoxic conditions, restoring the HIF-1 α level observed in normoxia.

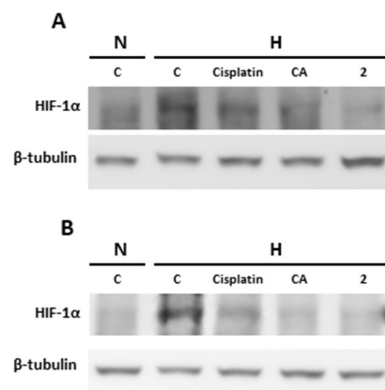


Figure 8. Effect of equitoxic treatments (48 h) with cisplatin, CA, and **2** on HIF-1 α protein level in A2780 (A) and HCT 116 (B) cells. C = control, N = normoxic conditions, H = hypoxic conditions. β -tubulin served as the loading control.

Conclusions

Cisplatin and CA show a synergistic antiproliferative activity. Their “combo” derivatives, namely the cisplatin-based Pt(IV) mono-CA **1** and especially di-CA **2**, offer excellent performances on a number of human tumor cell lines. This result relies mainly on the synergistic cellular accumulation of both drugs by virtue of the lipophilicity of the Pt(IV) conjugates. This is confirmed by the analysis of the gene expression in normoxia that is mainly influenced by the cytotoxic action of the released cisplatin, albeit a contribution of CA was observed as well. Both **1** and **2** are able to trigger apoptosis in a more efficient way than free cisplatin. The contribution of CA to the antiproliferative propensity of **2**, the most potent combo, is more evident under hypoxia. In fact, the released CA induces the HIF-1 α degradation thus augmenting the ability of **2** to bypass the well-known hypoxia-related cisplatin resistance.

Experimental

General procedures

$K_2[PtCl_4]$ and all other chemicals (Alfa Aesar and Sigma-Aldrich) were used without further purification. Complex (OC-6-44)-acetatodiamminedichloridohydroxidoplatinum(IV) (**0A**) was prepared according to an already published procedure.²⁶ The reactions under microwave irradiation were performed by using a CEM Discover® SP System equipped with a focused single mode and self-tuning cavity, an air cooling system, an automated power control based on temperature feedback, supplying power in 1 W increments from 0 to 300 W.

The purity of all the compounds was assessed by analytical RP-HPLC (see below), elemental analysis and determination of Pt content. Elemental analyses were carried out with an EA3000 CHN Elemental Analyzer (EuroVector, Milano, Italy). For all the compounds, the experimental values of the elemental analyses correspond to calculated values within

$\pm 0.4\%$. Platinum content determination was performed by inductively coupled plasma-optical emission spectrometry (ICP-OES Spectro Genesis equipped with a crossflow nebulizer, Spectro Analytical Instruments, Kleve, Germany) or inductively coupled plasma-mass spectrometry (ICP-MS, Thermo Optek X Series 2), accordingly to the platinum content of the sample and the sensitivity of the chosen instrument. Mineralization of the samples was performed by the addition of 70% w/w HNO_3 to each sample, followed by incubation for 1 h at 60 °C in an ultrasonic bath. Before the ICP-OES or ICP-MS measurements, the HNO_3 was diluted to a final 1% v/v concentration. In order to measure the platinum concentration by ICP-OES, the 299.797 nm line was selected. A Pt standard stock solution of 1000 mg L^{-1} was diluted in 1.0% v/v nitric acid to prepare calibration standards. Instrumental ICP-MS settings were optimized in order to yield maximum sensitivity for platinum. For quantitative determination, the most abundant isotopes of platinum and indium (used as internal standard) were measured at m/z 195 and 115, respectively.

The NMR spectra were measured on a NMR-Bruker Advance III operating at 500 MHz (^1H), 125.7 MHz (^{13}C) and 107.2 MHz (^{195}Pt with a spectral window of 2000 ppm), respectively. ^1H and ^{13}C NMR chemical shifts were reported in parts per million (ppm) referenced to solvent resonances. ^{195}Pt NMR spectra were recorded using a solution of $\text{K}_2[\text{PtCl}_4]$ in saturated aqueous KCl as the external reference. The shift for $\text{K}_2[\text{PtCl}_4]$ was adjusted to -1628 ppm from Na_2PtCl_6 ($\delta = 0$ ppm). ^{15}N NMR spectra were recorded using a solution of $^{15}\text{NH}_4\text{Cl}$ in 1 M HCl as the external reference. [^1H , ^{15}N] HSQC spectra (Heteronuclear Single Quantum Correlation) were obtained with the standard Bruker sequence hsqcetgpsiz with 0.2 s acquisition time, 8 scans, 1.3 s relaxation delay, and 128 F_1 points. DEPT-45 (Distortionless Enhancement by Polarization Transfer) spectra were recorded with 100 scans, 3.5 s relaxation delay, 0.5 s acquisition time and 75 Hz for $^1\text{J}(^{15}\text{N}, ^1\text{H})$.

Chromatographic analyses were carried out using a C18 Phenomenex Phenosphere-NEXT (5- μm , 250 \times 4.6 mm ID) column on a Waters HPLC-MS instrument (equipped with Alliance 2695 separations module, 2487 dual lambda absorbance detector, and 3100 mass detector). The UV-visible detector was set at 210 nm. Mass spectra were recorded using source and desolvation temperatures set to 150 and 250 °C, respectively, with nitrogen used both as a drying and as a nebulizing gas. The cone and the capillary voltages were usually +30 V (positive ion mode) or -30 V (negative ion mode) and 2.70 kV, respectively. Quasi-molecular ion peaks $[\text{M}+\text{H}]^+$, $[\text{M}+\text{Na}]^+$, $[\text{M}-\text{H}]^-$ and/or $[\text{M}+\text{Cl}]^-$ were assigned on the basis of the m/z values and of the simulated isotope distribution patterns.

Synthesis of the clofibroyl chloride (2-(4-chlorophenoxy)-2-methylpropanoyl chloride)

Clofibric acid (CA, 1 eq) was dissolved in dichloromethane and one drop of dimethylformamide (DMF), as catalyst, was added. While the solution was stirring, oxalyl dichloride (5 eq) was added dropwise and effervescence was observed. The reaction

mixture was stirred overnight at room temperature. The solvent and excess chloride were removed under reduced pressure (60 °C) to quantitatively yield a yellow/orange oil. Elemental analysis: found C, 51.22; H, 4.45. Calc. for $\text{C}_{10}\text{H}_{10}\text{Cl}_2\text{O}_2$ (233.09) C, 51.53; H, 4.32. ^1H NMR (500.13 MHz, $\text{DMSO}-d_6$): δ 1.64 (s, 6H, H5), 6.85 (d, 2H, H7, $^3J = 8.95$ Hz), 7.24 (d, 2H, H8, $^3J = 8.95$ Hz) ppm. ^{13}C NMR (125.76 MHz, $\text{DMSO}-d_6$): δ 25.1 (C5), 85.6 (C4), 121.2 (C7), 128.6 (C9), 129.6 (C8), 153.1 (C6), 178.3 (C1) ppm.

Synthesis of complex 1

The oily clofibroyl chloride previously obtained (1.33×10^{-3} mol, 10 eq) was dissolved in anhydrous acetone (3 mL) and added to a suspension of complex **OA** (0.05 g, 1.33×10^{-4} mol, 1 eq) in anhydrous acetone (2 mL). Excess pyridine (50 μL , 4 eq) was added dropwise to the reaction mixture which was then stirred and heated at reflux overnight. The bright yellow/orange solution was evaporated under reduced pressure and the resulting oil was treated with hexane, diethyl ether and finally water to yield 0.046 g (60%) of a yellowish powder for complex **1**. Elemental analysis: found C, 24.98; H, 3.37; N, 4.51; Pt, 34.22. Calc. for $\text{C}_{12}\text{H}_{19}\text{Cl}_3\text{N}_2\text{O}_5\text{Pt}$ (572.73) C, 25.17; H, 3.34; N, 4.89; Pt, 34.06. ^1H NMR (500.13 MHz, $\text{DMSO}-d_6$): δ 1.45 (s, 6H, H5), 1.93 (s, 3H, H1), 6.53 (m, 6H, NH_3), 6.90 (d, 2H, H7, $^3J = 8.90$ Hz), 7.20 (d, 2H, H8, $^3J = 8.95$ Hz) ppm. ^{13}C NMR (125.76 MHz, $\text{DMSO}-d_6$): δ 22.6 (C1), 25.7 (C5), 79.7 (C4), 120.7 (C7), 124.7 (C9), 128.6 (C8), 154.3 (C6), 177.9 (C2), 180.7 (C3) ppm. ^{195}Pt NMR (107.51 MHz, $\text{DMSO}-d_6$): δ 1208 ppm. ESI-MS (positive ion mode): 574.1 m/z . Calc. for $[\text{C}_{12}\text{H}_{20}\text{Cl}_3\text{N}_2\text{O}_5\text{Pt}]^+$ 573.7 m/z $[\text{M}+\text{H}]^+$.

Microwave assisted synthesis of complexes 1

A solution in anhydrous acetone of clofibroyl chloride (1.33×10^{-3} mol, 10 eq) was added in a microwave vessel to a suspension of complex **OA** (0.05 g, 1.33×10^{-4} mol, 1 eq) in anhydrous acetone to obtain a maximum volume of 5 mL. Excess pyridine (50 μL , 4 eq) was added dropwise to the stirring reaction mixture and the vessel was capped and introduced into the microwave cavity. The microwave unit was programmed to heat the vessel content to 55 °C over a 5-min ramp period and then hold at this temperature for 1 h; the power was automatically set at 50 W. During this time, the mixture was stirred with a magnetic bar. After heating, the vessel was allowed to cool to room temperature before removing it from the cavity. The solution obtained was transferred in a round bottomed flask and dried under vacuum. The resulting oil was treated with hexane, diethyl ether and then water to yield a yellowish powder. Yield: 0.052 g, 68%.

Microwave assisted synthesis of complex 0B

Cisplatin (0.083 g, 2.77×10^{-4} mol, 1 eq) was suspended in 4 mL of milliQ water in a microwave vessel and a wide excess of hydrogen peroxide 35% w/w (0.6 mL, 1.99×10^{-2} mol, 70 eq) was added dropwise. The vessel was capped and introduced into the microwave cavity. The microwave unit was programmed to heat the vessel content to 70 °C over a 5-min

ARTICLE

Dalton Transactions

ramp period and then hold at this temperature for 15 min; the power was automatically set at 15 W. During this time, the mixture was stirred with a magnetic bar. After heating, the vessel was allowed to cool to room temperature before removing it from the cavity. The solution obtained was transferred in a round bottomed flask and dried under vacuum. The resulting yellow oil was treated with ethanol first and then diethyl ether to yield a bright yellow powder (yield: 0.085 g, 92%). Elemental analysis: found H, 2.33; N, 8.45; Pt, 58.16. Calc. for $\text{Cl}_2\text{H}_8\text{N}_2\text{O}_2\text{Pt}$ (334.06) H, 2.41; N, 8.39; Pt, 58.40. ^{195}Pt NMR (107.51 MHz, D_2O): δ 860 ppm. ESI-MS (negative ion mode): 333.0 m/z $[\text{M}-\text{H}]^-$. Calc. for $[\text{Cl}_2\text{H}_7\text{N}_2\text{O}_2\text{Pt}]^-$ 332.9 m/z $[\text{M}-\text{H}]^-$.

Synthesis of complex 2

The oily acyl clofibroyl chloride (3.74×10^{-4} mol, 2.5 eq) was dissolved in anhydrous acetone (3 mL) and added to a suspension of 0.05 g (1.50×10^{-4} mol, 1 eq) of complex **OB** in anhydrous acetone (2 mL). Excess pyridine (50 μL , 2 eq) was added dropwise to the reaction mixture, which was then stirred and heated at reflux overnight. The yellow/orange suspension was dried under vacuum and the resulting oil was treated with hexane first, then with a solution 0.1 M of NaOH to eliminate the excess clofibric acid and finally water to yield 0.039 g (36%) of a yellowish powder. Elemental analysis: found C, 32.80; H, 3.29; N, 3.72; Pt 26.52. Calc. for $\text{C}_{20}\text{H}_{26}\text{Cl}_4\text{N}_2\text{O}_6\text{Pt}$ (727.32) C, 33.03; H, 3.60; N, 3.85; Pt, 26.82. ^1H NMR (500.13 MHz, $\text{DMSO}-d_6$): δ 1.46 (s, 12H, H_5), 6.56 (m, 6H, NH_3), 6.93 (d, 4H, H7, $^3J = 8.95$ Hz), 7.21 (d, 4H, H8, $^3J = 8.95$ Hz) ppm. ^{13}C NMR (125.76 MHz, $\text{DMSO}-d_6$): δ 25.7 (C5), 79.7 (C4), 120.9 (C7), 124.8 (C9), 128.6 (C8), 154.3 (C6), 180.6 (C3) ppm. ^{195}Pt NMR (107.51 MHz, $\text{DMSO}-d_6$): δ 1196 ppm. ESI-MS (positive ion mode): 728.3 m/z . Calc. for $[\text{C}_{20}\text{H}_{27}\text{Cl}_4\text{N}_2\text{O}_6\text{Pt}]^+$ 728.3 m/z $[\text{M}+\text{H}]^+$.

Microwave assisted synthesis of complex 2

A solution of clofibroyl chloride (3.74×10^{-4} mol, 2.5 eq) in anhydrous acetone was added in a microwave vessel to a suspension of complex **OB** (0.05 g, $1.50 \cdot 10^{-4}$ mol, 1 eq) in anhydrous acetone to obtain a maximum volume of 5 mL. Excess pyridine (50 μL , 2 eq) was added dropwise to the stirring reaction mixture and the vessel was capped and introduced into the microwave cavity. The microwave unit was programmed to heat the vessel content to 55 $^\circ\text{C}$ over a 5-min ramp period and then hold at this temperature for 1 h; the power was automatically set at 50 W. During this time, the mixture was stirred with a magnetic bar. After heating, the vessel was allowed to cool to room temperature before removing it from the cavity. The solution obtained was transferred in a round bottomed flask and dried under vacuum. The resulting oil was washed with hexane, then with a solution 0.1 M of NaOH to eliminate the excess clofibric acid, and finally with water to yield a yellowish powder. Yield: 0.041 g, 37%.

Synthesis of ^{15}N -containing complexes 1 and 2

The syntheses of complexes **1** and **2** containing ^{15}N ammonia were the same of those containing $^{14}\text{NH}_3$,^{25, 75} but starting from *cis*- $[\text{PtCl}_2(^{15}\text{NH}_3)_2]$.³¹ The relevant characterization data are reported below.

^{15}N -1. Elemental analysis: found C, 25.32; H, 3.11; N, 5.34; Pt, 33.67. Calc. for $\text{C}_{12}\text{H}_{19}\text{Cl}_3^{15}\text{N}_2\text{O}_5\text{Pt}$ (574.71) C, 25.08; H, 3.33; N, 5.22; Pt, 33.94. ^{15}N NMR (50.70 MHz, H_2O): δ -40.3 with satellite peaks at -37.7 ppm and -42.9 ppm ($^1J_{^{15}\text{N}-^{195}\text{Pt}} = 261.2$ Hz, $^2J_{^{15}\text{N}-^{195}\text{Pt}} = 55.0$ Hz) ppm. ESI-MS (positive ion mode): 576.0 m/z $[\text{M}+\text{H}]^+$. Calc. for $[\text{C}_{12}\text{H}_{20}\text{Cl}_3^{15}\text{N}_2\text{O}_5\text{Pt}]^+$ 575.7 m/z $[\text{M}+\text{H}]^+$.

^{15}N -2. Elemental analysis: found C, 32.70; H, 3.43; N, 4.32; Pt, 26.58. Calc. for $\text{C}_{20}\text{H}_{26}\text{Cl}_4^{15}\text{N}_2\text{O}_6\text{Pt}$ (729.31) C, 32.94; H, 3.59; N, 4.11; Pt, 26.75. ^{15}N NMR (50.70 MHz, H_2O): δ -39.8 ppm. ESI-MS (positive ion mode): 730.3 m/z $[\text{M}+\text{H}]^+$. Calc. for $[\text{C}_{20}\text{H}_{27}\text{Cl}_4^{15}\text{N}_2\text{O}_6\text{Pt}]^+$ 730.0 m/z $[\text{M}+\text{H}]^+$.

Solution behavior and reduction

The solution behavior of the investigated complexes (0.5 mM for complex **1**, 0.3 mM for complex **2**) was studied in 2 mM HEPES buffer (HEPES = 4-(2-hydroxyethyl)-1-piperazineethanesulfonic acid, pH = 7.5) with a variable amount of methanol (from 10% to 80% depending on the solubility of the complex) as a cosolvent along one week.

The reduction of the complexes (0.5 mM for complex **1** and ≤ 0.1 mM for complex **2**) with ascorbic acid (AA:Pt molar ratio = 10:1) was studied in HEPES (2 mM, pH 7.5)/MeOH 50/50 at 37 $^\circ\text{C}$. All these reactions were followed by monitoring the decrease of the area of the chromatographic peaks of the Pt complexes in HPLC-UV-MS. The mobile phase was a mixture of 15 mM aqueous HCOOH and CH_3OH in a ratio depending on the lipophilicity of the complex (aqueous formic acid/methanol 30/70 for **1**, 20/80 for **2**).

For ^{15}N NMR measurements, 20 μL of a 150-mM solution of **1** or saturated solution of **2** in DMF were diluted in 450 μL cell extract and D_2O (30 μL) was added (final D_2O content = 6%, final $[\text{Pt}] \leq 3$ mM) at 25 $^\circ\text{C}$. The complete cell extract was prepared according to literature procedures^{32, 76} by lysing 160 million A2780 ovarian cancer cells in 1.6 mL of deionized water followed by centrifugation to remove the insoluble material and by reducing the volume to 225 μL .

Lipophilicity and water solubility

Chromatographic analysis was used to evaluate the capacity factors of the compounds as reported elsewhere.^{40, 50, 77} Briefly, a chromatogram for each complex (0.5 mM) with eluant composition (15 mM formic acid/ CH_3OH 30/70) was run on a C18 column Phenosphere-NEXT (5- μm , 250 \times 4.6 mm ID). The corresponding retention time t_R was used to calculate $\log k'$ ($k' = (t_R - t_0) / t_0$); KCl was the internal reference to determine the column dead-time, t_0 .

The water solubility of the Pt(IV) complexes was determined preparing their saturated solution in ultrapure water, which were stirred in the dark at 25 $^\circ\text{C}$. After 24 h the solid residue was filtered off (0.20 μm cellulose filters) and the Pt content of the solutions was determined by means of ICP-OES.

Antiproliferative activity

The compounds under investigation were tested on a panel of commercial human cancer cell lines: ovarian endometrioid adenocarcinoma A2780 (ICLC HTL98008), colon carcinoma HCT 116 (ECACC 91091005), breast invasive ductal carcinoma MCF7 (ECACC 86012803), embryonal carcinoma of the testis NTERA-2 clone D1 (also known as NT2/D1, ICLC HTL97025), lung adenocarcinoma A549 (ICLC HTL03001), and biphasic malignant pleural mesothelioma (MPM) MSTO-211H (ICLC HL01018). Moreover, four cell lines derived from pleural effusions of untreated MPM patients were used: BR95 and MG06 (epithelioid phenotypes), MM98 (sarcomatoid phenotype) and its cisplatin-resistant subline MM98R derived from wild type by exposure to sub-lethal concentrations of cisplatin for several months.⁷⁸ The non-MPM cells and MSTO-211H were purchased from European Collection of Cell Cultures (ECACC, UK) or Interlab Cell Line Collection (ICLC, Genova, Italy), whereas the other MPM cell lines were obtained from the Hospital of Alessandria (Pathology Unit).

BR95 and MG06 cells were grown in Ham's F10 cell medium (GIBCO, Invitrogen Life Science, San Giuliano Milanese, Italy), DMEM (Sigma-Aldrich) was used for MSTO-211H, MM98 and MM98R, whereas A2780 NT2/D1 and A549 were grown in RPMI 1640, MCF7 in DMEM supplemented with non-essential aminoacids, and McCoy's 5A was used for HCT 116 cells. All media contained L-glutamine (2 mM), and were supplemented with penicillin (100 IU mL⁻¹), streptomycin (100 mg L⁻¹) and 10% heat inactivated fetal bovine serum (FBS). Cell culture and treatment were carried out at 37 °C in a 5% CO₂ humidified chamber. Cells were challenged with the compounds under study for 72 h of continuous treatment. Cisplatin was dissolved in 0.9% w/v NaCl aqueous solution brought to pH = 3 with HCl (final stock concentration 1 mM). The Pt(IV) complexes were dissolved in ethanol (final stock concentration 5 mM) and stored at -18 °C. The stock concentration was confirmed with ICP-OES measurements. The mother solutions were diluted in complete medium to the required concentration range and, where present, the total co-solvent concentration never exceeded 0.2% (this concentration was found to be non-toxic to the cells tested).

To assess the growth inhibition of the compounds under investigation, a cell viability test, *i.e.* the resazurin reduction assay, was used. Briefly, 2-5 × 10³ cells per well (depending on the cell line) were seeded in black sterile tissue-culture treated 96-well plates. At the end of the treatment, viability was assayed by 100 µg mL⁻¹ resazurin (Acros Chemicals, France) in fresh medium for 1 h at 37 °C, and the amount of the reduced product, resorufin, was measured by means of fluorescence (excitation λ = 535 nm, emission λ = 595 nm) with a Tecan Infinite F200Pro plate reader (Tecan, Austria).⁷⁹ In each experiment, cells were challenged with the drug candidates at different concentrations and the final data were calculated from at least three replicates of the same experiment performed in triplicate. The fluorescence of 8 wells containing medium without cells were used as a blank. Fluorescence data were normalized to 100% cell viability for non-treated cells.

Half-inhibiting concentration (IC₅₀), defined as the concentration of the drug reducing cell viability by 50%, was obtained from the dose-response sigmoid using Origin Pro (version 8, Microcal Software Inc., Northampton, MA, USA).

In order to verify the synergy between CA and cisplatin, A2780 cells were treated with increasing concentrations of cisplatin, CA, and a mixture cisplatin:CA in a fixed 1:1000 ratio, according to their respective IC₅₀ values. The experiment was repeated three times. According to the method of Chou and Talalay,^{45, 80, 81} the interaction between cisplatin and CA was computed in terms of combination index (*CI*) for non-mutually exclusive drugs by using the following equation:

$$CI = \frac{C1_m}{C1_a} + \frac{C2_m}{C2_a} + \frac{C1_m C2_m}{C1_a C2_a}$$

where *C1* and *C2* are the drug concentrations used in the mix (*C1_m* and *C2_m*) or alone (*C1_a* and *C2_a*) to obtain the same level of residual viability. Based on the actual experimental data, the *CI* values were calculated by solving the equation over an entire range of residual viability (from 5 to 95%, obtained from the sigmoidal regression). These data were then used to generate residual viability vs. *CI* plots, which is an effect-oriented means of presenting synergism or antagonism. Interpretation of *CI* values is defined such that *CI* = 1 indicates an additive effect, and *CI* < 1 and a *CI* > 1 indicate synergism and antagonism, respectively.

Cellular accumulation and DNA platination

A2780 cells were seeded in T25 flasks and allowed to grow until around 80% confluence. Then, the treatment was performed for 4 h with the complexes under investigations (10 µM) in complete medium. At time zero, 100 µL of medium was taken out from each sample to check the extracellular Pt concentration. At the end of the exposure, cells were washed three times with phosphate buffered saline (PBS), detached from the Petri dishes using 0.05% Trypsin 1X + 2% EDTA (HyClone, Thermo Fisher) and harvested in fresh complete medium. An automatic cell counting device (Countess®, Life Technologies), was used to measure the number and the mean diameter from every cell count. For cellular accumulation, about 5 × 10⁶ cells were transferred into a borosilicate glass tube and centrifuged at 1100 rpm for 5 min at room temperature. The supernatant was carefully removed by aspiration, while about 200 µL of the supernatant was left to limit the cellular loss. Cellular pellets were stored at -20 °C until mineralization and determination of the Pt content by ICP-MS.

The level of Pt found in cells after drug treatment and normalized upon the cell number (cellular Pt accumulation) was expressed as ng Pt per 10⁶ cells. The mean cellular volume, calculated from the actual mean cell diameter measured for every sample, was used to obtain the cellular Pt concentration. The ratio between the cellular and extracellular (in the culture medium) concentrations is defined as accumulation ratio, AR.⁸²

For DNA platination measurement,³ about 10 × 10⁶ cells were transferred into a plastic tube and centrifuged at 1100

rpm for 5 min at room temperature. The supernatant was removed by aspiration and the cell pellet stored at $-20\text{ }^{\circ}\text{C}$ until the total genomic DNA extraction with a commercial kit (GenUP™ gDNA kit, Biotechnrabit, Hennigsdorf, Germany). According to the manufacturer's instructions, during cell lysis, DNA was purified employing RNase A and proteinase K, then extracted on silica centrifugation columns. After washing, DNA was eluted in 300 μL of elution buffer. The sample (8 μL) and the same amount of elution buffer (blank) were diluted in TE buffer (10 mM Tris-HCl, 1 mM EDTA, pH 8.0) to 80 μL , to fit 0.5 cm path length in UV-transparent microplates half-area wells (UV-Star®, Greiner Bio-one). Absorbance at 260 nm (A_{260} , relative to nucleic acids) and 280 nm (A_{280} , relative to proteins) were recorded from triplicate wells with a Tecan Infinite F200Pro plate reader (Tecan, Austria). For each measurement, A_{260} and A_{280} were corrected by subtraction of the background, then the purity of the samples was verified by means of the A_{260} to A_{280} ratio, that always resulted >2 . After the subtraction of mean A_{260} of blank wells, the DNA concentration was computed from the corrected A_{260} by means of a calibration curve based on calf thymus DNA: an absorbance of 1 unit at 260 nm corresponds to 100 μg of DNA per mL. The remaining DNA elution buffer was transferred into a borosilicate glass tube, weighted to compute the total amount of DNA, and then stored at $-20\text{ }^{\circ}\text{C}$ until mineralization. Mineralization and subsequent Pt content determination were performed as above-mentioned for the whole cells. The amount of Pt bound to DNA was expressed as pg of Pt per μg of DNA experimentally found.

Caspase-3/7 activity

The assay was performed on A2780 cells similarly to a previous report,⁷⁹ though with some modifications. Briefly, 2×10^5 cells were seeded in 96-well black tissue culture (TC) plates in complete medium, the day before treatment with the complexes at different concentrations. After 24 h, cells were washed and lysed with 25 μL of lysis buffer (10 mM HEPES, 2 mM EDTA, 2 mM DTT, 0.1 % CHAPS, pH 7.4). The caspase 3/7 inhibitor *N*-Ac-Asp-Glu-Val-Asp-CHO (Ac-DEVD-CHO) 10 mM (Sigma-Aldrich) was added to control wells (data not shown). Then, 200 μL the caspase-3 fluorescent substrate, Ac-DEVD-AFC (Sigma-Aldrich), 100 mM in lysis buffer, was added to all the wells. The activity was followed for 30 min by means of fluorescence at excitation $\lambda = 390\text{ nm}$, emission $\lambda = 520\text{ nm}$, normalized vs. the blank. Data were normalized to residual viability and final fold activity (with respect to control wells) was calculated as the mean of at least three independent replicates performed in duplicate for each condition.

Hoechst 33342 staining

A2780 cells (2×10^5) were seeded on Nunc™ Lab-Tek™ 4-chamber slides and allowed to attach for 24 h. The following day, the treatment was added to a final concentration of 1 mM CA, 1 μM **1** and **2**. After 24 h, the medium was replaced with the staining solution, consisting of 5 ng mL^{-1} Hoechst 33342 in Earle's Balanced Salt solution (EBSS). Cells were incubated in the dark for 5 min, washed thrice with EBSS and immediately

observed using a standard DAPI filter set (excitation $\lambda = 350\text{ nm}$, emission $\lambda = 461\text{ nm}$) of a fluorescence microscope (Zeiss Axiolab), equipped with a digital photo camera (Nikon digital Sights, DS-U3). Pictures were taken at 20X magnification.

Quantitative Reverse Transcription PCR (RT-qPCR)

A2780 cells (2×10^6) were seeded on T25 flasks and allowed to attach for 24 h. The treatment was performed with equitoxic concentrations (*i.e.* 6 μM complex **1**, 2 μM complex **2**, 30 μM cisplatin, and 5 mM CA). After 24 h, RNA was extracted and purified by DNase treatment with a commercial kit (RNASPIN MINI, GE Healthcare); then it was quantified and checked for purity by means of absorbance at $\lambda = 260, 280,$ and 340 nm in UV-Star half area UV transparent plate (Brand) with the above-mentioned microplate reader. For each sample, 1 μg of RNA was retrotranscribed (RT) to cDNA with the Revertaid cDNA First strand kit (Thermo-Fisher) using random hexamer primers at $45\text{ }^{\circ}\text{C}$, following the manufacturer's instructions. qPCR was performed in triplicate on each sample (10 ng) to detect the expression levels of ACOX1, CPT1A, p53, p21, Cyclin D1, E, HMOX1, and the reference genes RNA18S, HPRT1, GAPDH. Primer sequences were designed using the NCBI tool and checked for target specificity including splice variants; they are reported in Table S1 (see ESI). Reactions were based on the SsoFast EvaGreen Supermix (Bio-Rad) in the presence of 0.4 μM primer pairs except for RNA18S (0.2 μM), according to the manufacturer's instructions, in a reaction volume of 10 μL . In order to compute reaction efficiency, a standard curve was performed for each master mix. qPCR was performed in triplicate using and the CFX368 thermal cycler (Bio-Rad). The reaction conditions were $95\text{ }^{\circ}\text{C}$ for 1 min, followed by 45 cycles $98\text{ }^{\circ}\text{C}$ for 5 seconds and anneal–extend step for 5 seconds at $60\text{ }^{\circ}\text{C}$, with data collection. At the end of these cycles, a melting curve ($65\text{ }^{\circ}\text{C}$ to $95\text{ }^{\circ}\text{C}$, with plate read every $0.5\text{ }^{\circ}\text{C}$) was performed in order to assess the specificity of the amplification product by single peak melting temperature verification. Results were normalized on the reference genes and on the control according to the $\Delta\Delta\text{C}_q$ method. All data analyses were performed with the built-in software (CFX Manager, Bio-Rad).

ROS assay

The 2',7'-dichlorofluorescein diacetate ($\text{H}_2\text{DCF-DA}$) dye was used to detect reactive oxygen species (ROS) levels. 2×10^5 A2780 cells were seeded in black sterile 96-well TC plates the day before treatment (8 wells/treatment), performed the following day, to a final concentration of 1 mM CA, 1 μM cisplatin, **1** and **2**. After 24h, 3 wells of each treatment were used to assess residual viability by means of the resazurin reduction assay, while the remaining wells were loaded with 10 μM $\text{H}_2\text{DCF-DA}$ in EBSS at $37\text{ }^{\circ}\text{C}$ for 30 min, in the dark. Immediately before the end of loading H_2O_2 5 mM (final concentration) was added as positive control, while a control column received 10 mM *N*-acetylcysteine (NAC), a well-known anti-oxidant, as negative control of each condition (data not shown). After 2 washes by EBSS, oxidized DCF fluorescence

was measured at excitation $\lambda = 485$ nm and emission $\lambda = 535$ nm. Data were normalized on viability.

Hypoxia vs. normoxia

Hypoxia was induced by placing the cells for 48 h into a modular incubator chamber (Billups Rothenberg Inc., Del Mar, CA, USA) flushed with a mixture of 1% O₂, 5% CO₂ and 94% N₂ at 37 °C. The antiproliferative effect was assessed using the (3-(4,5-dimethylthiazolyl-2)-2,5-diphenyltetrazolium bromide (MTT) assay.⁸³ Briefly, 3×10^3 cells per well were seeded onto 96-wells plate and allow to grow for 24 h prior to the treatment with the drugs and placed under normoxic and hypoxic conditions for 48 h. At the end of treatment, MTT was added to each well (final concentration 0.4 mg mL⁻¹) and left reacting for 3 h at 37 °C. The formazan crystals, formed through MTT metabolism by viable cells, were dissolved in DMSO and the optical densities were measured at $\lambda = 570$ nm using a Universal Microplate Reader EL800 (Bio-Tek Instruments). IC₅₀ values were obtained by nonlinear regression analysis, using the GraphPad PRISM 3.03 software (GraphPad Software Inc., San Diego CA, USA).

Flow cytometric analysis

The effects of CA, **1**, and **2** on apoptotic cell death induction and cell cycle distribution were evaluated using propidium iodide (PI) staining following 48 h-exposure under normoxic and hypoxic conditions. The drugs were administered at their respective IC₅₀ values (as assessed on normoxic cells). A Becton Dickinson FACScalibur instrument equipped with a 15 mW, $\lambda = 488$ nm, air-cooled argon laser was employed. Data were analyzed using Cell Quest Pro software (Becton Dickinson). Cells were fixed in 0.5 mL of ice-cold 70% ethanol and stored at -20 °C. Cells were then centrifuged, washed with PBS, resuspended in the dyeing solution (50 μ g mL⁻¹ PI, 20 μ g mL⁻¹ RNase in 1 \times PBS) and analyzed. The percentage of apoptotic cells in each sample was determined based on the sub-G1 peaks detected in monoparametric histograms.

Assessment of HIF-1 α expression by Western blot analysis

Western blot analysis was carried out to detect the expression of HIF-1 α in whole cell lysates, following normoxic or hypoxic incubation, with or without drug treatment. A2780 and HCT 116 cancer cells were treated for 48 h with cisplatin, CA, and **2** at their respective IC₅₀, under hypoxic conditions. At the end of the treatment, cells were lysed in a lysis buffer (NaCl 120 mM; NaF 25 mM; EDTA 5 mM; EGTA 6 mM; sodium pyrophosphate 25 mM in Tris-buffered saline buffer, TBS, 20 mM pH 7.4; phenylmethylsulfonyl fluoride, PMSF, 2 mM; Na₃VO₄ 1 mM; phenylarsine oxide 1 mM; 1% nonyl phenoxypolyethoxyethanol, NP-40, and 10% Protease Inhibitor Cocktail). Protein concentration was determined by the BCA assay (Pierce, Italy) and 80 μ g of protein per sample were loaded onto polyacrylamide gels (8%) and separated under denaturing conditions. Protein bands were then transferred onto Hybond-P membranes (Amersham Biosciences, Italy) and Western blot analysis was performed by standard techniques with mouse monoclonal anti-human HIF-

1 α antibody (BD Biosciences). Equal loading of the samples was verified by re-probing the blots with a mouse monoclonal anti- β -tubulin antibody (Sigma Aldrich). Protein bands were visualized using a peroxidase-conjugated anti-mouse secondary antibody and the Westar Supernova kit (Cyagen).

Conflicts of interest

There are no conflicts of interest to declare.

Acknowledgements

We thank Compagnia di San Paolo (Torino) within the research project BIPLANES. We are indebted to Inter-University Consortium for Research on the Chemistry of Metals in Biological Systems (CIRCMSB, Bari) for providing opportunities of stimulating discussion.

Notes and references

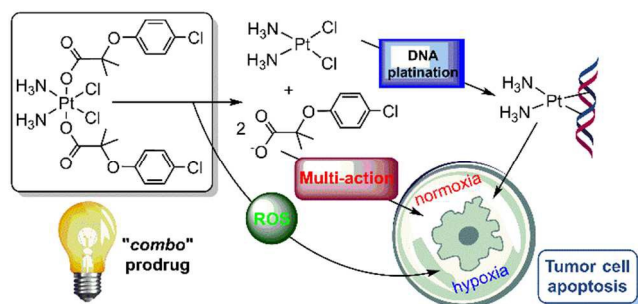
1. R. Morphy, C. Kay and Z. Rankovic, *Drug Discovery Today*, 2004, **9**, 641-651.
2. L. K. Bai, C. Z. Gao, Q. H. Liu, C. T. Yu, Z. X. Zhang, L. X. Cai, B. Yang, Y. X. Qian, J. Yang and X. L. Liao, *European Journal of Medicinal Chemistry*, 2017, **140**, 349-382.
3. E. Gabano, M. Ravera, I. Zanellato, S. Tinello, A. Gallina, B. Rangone, V. Gandin, C. Marzano, M. G. Bottone and D. Osella, *Dalton Transactions*, 2017, **46**, 14174-14185.
4. A. Najjar, N. Rajabi and R. Karaman, *Current Pharmaceutical Design*, 2017, **23**, 2366-2376.
5. E. Gabano, M. Ravera and D. Osella, *Dalton Transactions*, 2014, **43**, 9813-9820.
6. T. C. Johnstone, K. Suntharalingam and S. J. Lippard, *Chemical Reviews*, 2016, **116**, 3436-3486.
7. M. D. Hall, H. R. Mellor, R. Callaghan and T. W. Hambley, *Journal of Medicinal Chemistry*, 2007, **50**, 3403-3411.
8. E. Wexselblatt and D. Gibson, *Journal of Inorganic Biochemistry*, 2012, **117**, 220-229.
9. D. Gibson, *Dalton Transactions*, 2016, **45**, 12983-12991.
10. R. Raveendran, J. P. Braude, E. Wexselblatt, V. Novohradsky, O. Stuchlikova, V. Brabec, V. Gandin and D. Gibson, *Chemical Science*, 2016, **7**, 2381-2391.
11. F. Penna, G. Bonelli, F. M. Baccino and P. Costelli, *Current Medicinal Chemistry*, 2010, **17**, 309-320.
12. Y. Yokoyama, B. Xin, T. Shigeto, M. Umemoto, A. Kasai-Sakamoto, M. Futagami, S. Tsuchida, F. Al-Mulla and H. Mizunuma, *Molecular Cancer Therapeutics*, 2007, **6**, 1379-1386.
13. J. D. Zhou, S. Y. Zhang, J. Xue, J. Avery, J. C. Wu, S. E. Lind and W. Q. Ding, *Journal of Biological Chemistry*, 2012, **287**, 35161-35169.
14. G. L. Semenza, *Cell*, 2012, **148**, 399-408.
15. S. Unwith, H. L. Zhao, L. Hennah and D. Q. Ma, *International Journal of Cancer*, 2015, **136**, 2491-2503.
16. E. Monti and M. B. Gariboldi, *Current Molecular Pharmacology*, 2011, **4**, 62-77.
17. Z. C. Xu, J. Zhao, S. H. Gou and G. Xu, *Chemical Communications*, 2017, **53**, 3749-3752.

ARTICLE

Dalton Transactions

18. H. R. Mellor, S. Snelling, M. D. Hall, S. Modok, M. Jaffar, T. W. Hambley and R. Callaghan, *Biochemical Pharmacology*, 2005, **70**, 1137-1146.
19. E. Schreiber-Brynzak, V. Pichler, P. Heffeter, B. Hanson, S. Theiner, I. Lichtscheidl-Schultz, C. Kornauth, L. Bamonti, V. Dhery, D. Groza, D. Berry, W. Berger, M. Galanski, M. A. Jakupec and B. K. Keppler, *Metallomics*, 2016, **8**, 422-433.
20. S. Goschl, E. Schreiber-Brynzak, V. Pichler, K. Cseh, P. Heffeter, U. Jungwirth, M. A. Jakupec, W. Berger and B. K. Keppler, *Metallomics*, 2017, **9**, 309-322.
21. S. Y. Li, N. Gokden, M. D. Okusa, R. Bhatt and D. Portilla, *American Journal of Physiology-Renal Physiology*, 2005, **289**, F469-F480.
22. P. Thongnuanjan, S. Soodvilai and V. Chatsudthipong, *Journal of Toxicological Sciences*, 2016, **41**, 339-349.
23. S. C. Dhara, *Indian Journal of Chemistry*, 1970, **8**, 193-194.
24. F. D. Rochon and L. M. Gruia, *Inorganica Chimica Acta*, 2000, **306**, 193-204.
25. J. Z. Zhang, P. Bonnitza, E. Wexselblatt, A. V. Klein, Y. Najajreh, D. Gibson and T. W. Hambley, *Chemistry-a European Journal*, 2013, **19**, 481-483.
26. M. Ravera, E. Gabano, I. Zanellato, F. Fregonese, G. Pelosi, J. A. Platts and D. Osella, *Dalton Transactions*, 2016, **45**, 5300-5309.
27. E. Petruzzella, C. V. Chiroasca, C. S. Heidenga and J. D. Hoeschele, *Dalton Transactions*, 2015, **44**, 3384-3392.
28. E. A. Pedrick and N. E. Leadbeater, *Inorganic Chemistry Communications*, 2011, **14**, 481-483.
29. E. Gabano, S. Gama, F. Mendes, F. Fregonese, A. Paulo and M. Ravera, *Inorganica Chimica Acta*, 2015, **437**, 16-19.
30. E. Gabano, E. Perin, C. Fielden, J. A. Platts, A. Gallina, B. Rangone and M. Ravera, *Dalton Transactions*, 2017, **46**, 10246-10254.
31. M. S. Davies, M. D. Hall, S. J. Berners-Price and T. W. Hambley, *Inorganic Chemistry*, 2008, **47**, 7673-7680.
32. A. Nemirovski, Y. Kasherman, Y. Tzaraf and D. Gibson, *Journal of Medicinal Chemistry*, 2007, **50**, 5554-5556.
33. D. Gibson, *Dalton Transactions*, 2009, 10681-10689.
34. P. S. Pregosin, *Coordination Chemistry Reviews*, 1982, **44**, 247-291.
35. T. G. Appleton, J. R. Hall and S. F. Ralph, *Inorganic Chemistry*, 1985, **24**, 673-677.
36. S. J. Berners-Price, L. Ronconi and P. J. Sadler, *Progress in Nuclear Magnetic Resonance Spectroscopy*, 2006, **49**, 65-98.
37. E. Gabano, E. Marengo, M. Bobba, E. Robotti, C. Cassino, M. Botta and D. Osella, *Coordination Chemistry Reviews*, 2006, **250**, 2158-2174.
38. L. Ronconi and P. J. Sadler, *Coordination Chemistry Reviews*, 2008, **252**, 2239-2277.
39. P. Gramatica, E. Papa, M. Luini, E. Monti, M. B. Gariboldi, M. Ravera, E. Gabano, L. Gaviglio and D. Osella, *Journal of Biological Inorganic Chemistry*, 2010, **15**, 1157-1169.
40. G. Ermondi, G. Caron, M. Ravera, E. Gabano, S. Bianco, J. A. Platts and D. Osella, *Dalton Transactions*, 2013, **42**, 3482-3489.
41. A. C. Tsipis and I. N. Karapetsas, *Dalton Transactions*, 2014, **43**, 5409-5426.
42. V. Novohradsky, L. Zerzankova, J. Stepankova, O. Vrana, R. Raveendran, D. Gibson, J. Kasparkova and V. Brabec, *Biochemical Pharmacology*, 2015, **95**, 133-144.
43. M. Ravera, E. Gabano, I. Zanellato, A. Gallina, E. Perin, A. Arrais, S. Cantamessa and D. Osella, *Dalton Transactions*, 2017, **46**, 1559-1566.
44. T. C. Chou and P. Talalay, *European Journal of Biochemistry*, 1981, **115**, 207-216.
45. T. C. Chou and P. Talalay, *Advances in Enzyme Regulation*, 1984, **22**, 27-55.
46. Z. H. Siddik, *Oncogene*, 2003, **22**, 7265-7279.
47. L. Galluzzi, L. Senovilla, I. Vitale, J. Michels, I. Martins, O. Kepp, M. Castedo and G. Kroemer, *Oncogene*, 2012, **31**, 1869-1883.
48. S. Tone, K. Sugimoto, K. Tanda, T. Suda, K. Uehira, H. Kanouchi, K. Samejima, Y. Minatogawa and W. C. Earnshaw, *Experimental Cell Research*, 2007, **313**, 3635-3644.
49. M. Ravera, E. Gabano, I. Zanellato, I. Bonarrigo, M. Alessio, F. Arnesano, A. Galliani, G. Natile and D. Osella, *Journal of Inorganic Biochemistry*, 2015, **150**, 1-8.
50. J. A. Platts, G. Ermondi, G. Caron, M. Ravera, E. Gabano, L. Gaviglio, G. Pelosi and D. Osella, *Journal of Biological Inorganic Chemistry*, 2011, **16**, 361-372.
51. I. V. Tetko, H. P. Varbanov, M. Galanski, M. Talmaciu, J. A. Platts, M. Ravera and E. Gabano, *Journal of Inorganic Biochemistry*, 2016, **156**, 1-13.
52. C. M. Riley and L. A. Sternson, in *Analytical Profiles of Drug Substances*, ed. F. Klaus, Academic Press, 1985, vol. Volume 14, pp. 77-105.
53. J. P. Souchard, T. T. B. Ha, S. Cros and N. P. Johnson, *Journal of Medicinal Chemistry*, 1991, **34**, 863-864.
54. M. Yoshida, A. R. Khokhar and Z. H. Siddik, *Cancer Research*, 1994, **54**, 4691-4697.
55. D. Screnci, M. J. McKeage, P. Galettis, T. W. Hambley, B. D. Palmer and B. C. Baguley, *British Journal of Cancer*, 2000, **82**, 966-972.
56. M. D. Hall, S. Amjadi, M. Zhang, P. J. Beale and T. W. Hambley, *Journal of Inorganic Biochemistry*, 2004, **98**, 1614-1624.
57. I. V. Tetko, I. Jaroszewicz, J. A. Platts and J. Kuduk-Jaworska, *Journal of Inorganic Biochemistry*, 2008, **102**, 1424-1437.
58. E. Lindauer and E. Holler, *Biochemical Pharmacology*, 1996, **52**, 7-14.
59. M. Alessio, I. Zanellato, I. Bonarrigo, E. Gabano, M. Ravera and D. Osella, *Journal of Inorganic Biochemistry*, 2013, **129**, 52-57.
60. S. Wang, B. N. Hannafon, J. D. Zhou and W. Q. Ding, *Cellular Physiology and Biochemistry*, 2013, **32**, 1255-1264.
61. P. D. McMullen, S. Bhattacharya, C. G. Woods, B. Sun, K. Yarborough, S. M. Ross, M. E. Miller, M. T. McBride, E. L. LeCluyse, R. A. Clewell and M. E. Andersen, *Chemico-Biological Interactions*, 2014, **209**, 14-24.
62. K. Chandran, S. Goswami and N. Sharma-Walia, *Oncotarget*, 2016, **7**, 15577-15599.
63. J. Cmielova and M. Rezacova, *Journal of Cellular Biochemistry*, 2011, **112**, 3502-3506.
64. I. Zanellato, I. Bonarrigo, M. Sardi, M. Alessio, E. Gabano, M. Ravera and D. Osella, *ChemMedChem*, 2011, **6**, 2287-2293.
65. P. Vaupel and A. Mayer, *Cancer and Metastasis Reviews*, 2007, **26**, 225-239.

66. J. A. Bertout, S. A. Patel and M. C. Simon, *Nature Reviews Cancer*, 2008, **8**, 967-975.
67. S. Cipro, J. Hrebackova, J. Hrabeta, J. Poljakova and T. Eckschlager, *Oncology Reports*, 2012, **27**, 1219-1226.
68. J. Adamski, A. Price, C. Dive and G. Makin, *Plos One*, 2013, **8**.
69. X. R. Song, X. X. Liu, W. L. Chi, Y. L. Liu, L. Wei, X. W. Wang and J. M. Yu, *Cancer Chemotherapy and Pharmacology*, 2006, **58**, 776-784.
70. S. Koch, F. Mayer, F. Honecker, M. Schittenhelm and C. Bokemeyer, *British Journal of Cancer*, 2003, **89**, 2133-2139.
71. S. Strese, M. Fryknas, R. Larsson and J. Gullbo, *Bmc Cancer*, 2013, **13**.
72. G. Laurenti, E. Benedetti, B. D'Angelo, L. Cristiano, B. Cinque, S. Raysi, M. Alecci, M. P. Ceru, M. G. Cifone, R. Galzio, A. Giordano and A. Cimini, *Journal of Cellular Biochemistry*, 2011, **112**, 3891-3901.
73. R. Galzio, L. Cristiano, A. Fidoamore, M. G. Cifone, E. Benedetti, B. Cinque, P. Menghini, S. R. Dehcordi, R. Ippoliti, A. Giordano and A. Cimini, *Journal of Cellular Biochemistry*, 2012, **113**, 3342-3352.
74. X. J. Lin, K. Ramamurthi, M. Mishima, A. Kondo, R. D. Christen and S. B. Howell, *Cancer Research*, 2001, **61**, 1508-1516.
75. G. Pelosi, M. Ravera, E. Gabano, F. Fregonese and D. Osella, *Chemical Communications*, 2015, **51**, 8051-8053.
76. A. Nemirovski, I. Vinograd, K. Takroui, A. Mijovilovich, A. Rompel and D. Gibson, *Chemical Communications*, 2010, **46**, 1842-1844.
77. J. A. Platts, S. P. Oldfield, M. M. Reif, A. Palmucci, E. Gabano and D. Osella, *Journal of Inorganic Biochemistry*, 2006, **100**, 1199-1207.
78. I. Zanellato, C. D. Boidi, G. Lingua, P. G. Betta, S. Orecchia, E. Monti and D. Osella, *Cancer Chemotherapy and Pharmacology*, 2011, **67**, 265-273.
79. M. Ravera, E. Gabano, S. Bianco, G. Ermondi, G. Caron, M. Vallaro, G. Pelosi, I. Zanellato, I. Bonarrigo, C. Cassino and D. Osella, *Inorganica Chimica Acta*, 2015, **432**, 115-127.
80. T.-C. Chou, *Pharmacological Reviews*, 2006, **58**, 621-681.
81. T. C. Chou, *Cancer Research*, 2010, **70**, 440-446.
82. A. Ghezzi, M. Aceto, C. Cassino, E. Gabano and D. Osella, *Journal of Inorganic Biochemistry*, 2004, **98**, 73-78.
83. D. A. Scudiero, R. H. Shoemaker, K. D. Paull, A. Monks, S. Tierney, T. H. Nofziger, M. J. Currens, D. Seniff and M. R. Boyd, *Cancer Research*, 1988, **48**, 4827-4833.



The cisplatin/clofibrato combos are multi-action Pt(IV) complexes active on a panel of human tumor cell lines, also in hypoxic conditions